SYMMETRICAL RESTRICTIONS ON THE IMPLEMENTATION OF HYDROCARBON CHAINS OF PHOSPHOLIPIDS OF BIOMEMBRANES AND ALPHA HELIX

A. L. Talis*

Nesmeyanov Institute of Organoelement Compounds, Russian Academy of Sciences, ul. Vavilova 28, str. 1, Moscow, 119334 Russia

Abstract

The symmetry restrictions are presented that allow for determining ideal prototypes of hydrocarbon chains of biomembrane phospholipids and α-helix. Prototypes are established by partitions of linear substructures of 4D polyhedra into building units determined by minimal finite projective geometry.

Key words: hydrocarbon chains of biomembrane phospholipids, α-helix, non-crystallographic symmetry.
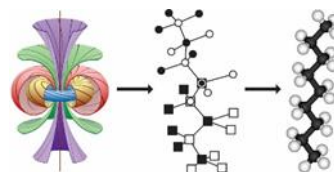
Introduction

In hydrocarbon chains of biomembrane phospholipids, the combinations of N (number of carbon atoms), d (number of double bonds), and ω (position of the first double bond relative to the terminal CH_3 group) comprise a huge number of theoretically possible variants. However, there are realizations in biomembranes of 20–30 sets (N, d, ω) of chains of definite structure [1]. Let us show that a realized set (N, d, ω) is subject to symmetry restrictions: the chain is assembled from a certain number of building units and is imbedded in a 4D polyhedron corresponding to the coordination number of four for carbon. The same restrictions also determine the structure of the α-helix.

Results and discussion

The surface of a biomembrane is determined by the minimal surface in the 3D sphere S^3 positioned in the 4D Euclidean space E^4 [2] and projected into a system of coaxial tori in E^3. In a physically admissible approximation, the saturated moieties of hydrocarbon chains are tetra-coordinated. Hence, for adequate descriptions of the chains in question, it is necessary to make transition from S^3 to its maximally symmetric discrete substructure of centered regular tetrahedra. Such a substructure is a 4D 720-vertex polytope {720} that arises upon centering of each of the 600 regular tetrahedra in the 120-vertex "white" polytope {3,3,5}—an analog of the icosahedron (Fig. 1a) in E^4. Then 600 "black" vertices in the centers of the tetrahedra belong to the polytope {5,3,3}—an analog of the dodecahedron (Fig. 1b) in E^4 [3, 4]. The group of rotations of the polytopes {3,3,5}, {5,3,3} and {720} is the group ± [I x I], where I is the group of rotations of the icosahedron [5]. The hydrocarbon chain of the phospholipid must be embedded in the linear substructure {720}: the white tetrahelix from {3,3,5}, a series of vertices of which centers the black tetrahedra from {5,3,3}. The tetrahelix [6] is a partition of a 30-vertex torus into 30 tetrahedra (Fig. 2)
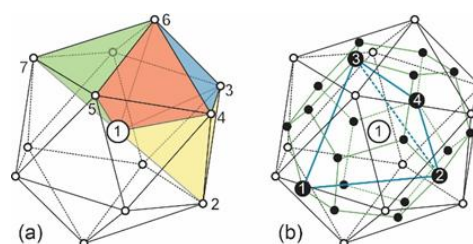

Figure 1. (*a*) Green, red, blue, and yellow tetrahedra from icosahedron form a 7-vertex tetrablock. (*b*) In icosahedron (*a*) the dodecahedron is included, four vertices of which determine a tetrahedron. The common center of all constructions is shown as a large circle.

with the screw axis 30/11 performing the rotations by 11·360°/30 = 132° [4].

In the polytope {3,3,5}, the Gosset's construction [4] allows us to partition the tetrahelix into 6 quadruples of tetrahedra (tetrablocks) that include all its vertices and adjoin each other by edges (Fig. 2). The tetrablock (TB, T-block) is a seven-vertex union of four face-sharing regular tetrahedra (Figs. 1a, 2). The graph TB is given by the minimal finite projective geometry PG(2,2); therefore, T-block is the building unit for the structures approximated by the union of regular tetrahedra [7]. The center of each of the 6 TB in the tetrahelix (Fig. 2) is the center of the white icosahedron in {720} (Fig. 1a) as well as the black dodecahedron included in it, and therefore also of the black tetrahedron (Fig. 1b). The union of the white TB and the black tetrahedron determines a 7+4 = 11-vertex decorated tetrablock (DTB). In the union of two DTBs, the shared edge of their white T-blocks traverses the center of a pentagon of the black dodecahedron that borders the black dodecahedra, whose centers
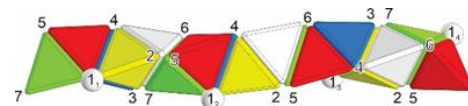

Figure 2. Partition of tetrahelix into (united by coincident edges 2-3 and 5-7) tetrablocks (Fig. 1a) and white tetrahedra not belonging to them.

are the centers of these white TBs (Fig. 3a). A diagonal of this pentagon joins black tetrahedra and (upon discarding the shared edge of the united white T-blocks and the "C"–"H"-vertex realization) determines the double bond in the hydrocarbon chain (Fig. 3b). Such a union of 2 DTBs (one of them being terminal in the chain) corresponds to the position ω3 of this double bond (Fig. 3b). In the polytope {720} such a union of DTBs leads to a closure of the chain of the 6 DTBs inside the torus (Fig. 3a). This correlates with an experimentally established restriction d ≤ 6 for (poly)unsaturated chains. In this case, there is only one methylene group CH_2 between each pair of double bonds (Fig. 3b).
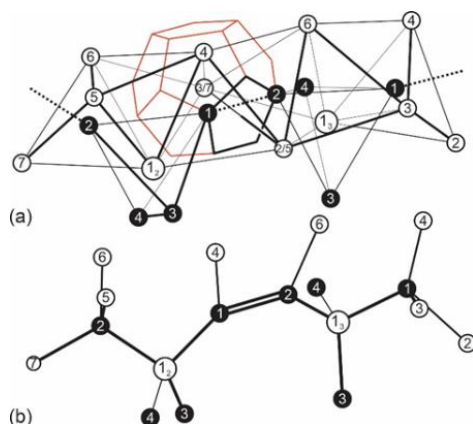

Figure 3. (*a*) Decorated tetrablocks of black tetrahedra and white tetrablocks with centers in 1_2 and 1_3 (Fig. 2) are united by edge 2/5-3/7. It goes through pentagon of dodecahedron whose diagonal joins black tetrahedra. (*b*) Discarding edge 2/5-3/7 in (*a*) determines double bond in hydrocarbon chain of biomembranes.

The union (by a 2-fold axis) of the white and black TBs leads to a 14-vertex composite tetrablock (CTB) that upon the "C"–"H" realization of vertices becomes a fragment of the saturated hydrocarbon chain. Hence, the union of adjacent CTBs by two vertices (vertices of the same color coincide) leads to the i·(14-2)-vertex chains i = 3, 4, 5 of the types $-C_{12}H_{24}-$, $-C_{16}H_{32}-$, and $-C_{20}H_{40}-$, respectively. In the general case, the chains in question correspond to a "mixed" variant of the union of CTBs and/or DTBs: both by two vertices and by (then discarded) end edges. For instance, the union of 2 DTBs by 2 vertices, and then with the third DTB by an end edge corresponds to the ω6 configuration in the hydrocarbon chain.

Determination of sets (N, d, ω) corresponding to the union of a whole number of CTBs and/or DTBs, embedded in a linear substructure of the polytope {720}, is necessary for an a priori determination of hydrocarbon chains of biomembrane phospholipids allowed by symmetry and for their adequate classification. Moreover, the symmetry (non-crystallographic group) of the chain can correlate with its importance in structural organization and properties of the biomembrane. Let us emphasize that satisfying symmetry restrictions is just a necessary but not sufficient condition for the existence of a chain that may not be realized under given physical conditions.

The efficacy of the present approach is substantiated by a selection of the helix of the whole number of TBs with the 40/11 screw axis (rotation by 11·360°/40 = 99°). The realization of the same helix {40/11} as the helix of atoms C_α in the α-helices of various proteins allows one to explain the universal nature of the

α-helix and its experimentally determined rotation angle of (99±1)° instead of 100° according to Pauling [8, 9].

The linear substructure (of 40 prismatic cells) of the polytope with the group of symmetry ±[O×D_{20}] also possesses the axis 40/11. This polytope is defined in a family of tube polytopes with symmetry groups $1/2[O×C_{2n}]$, n = 14, 18, 5, 22, 12, 7 for n = 5 and for the center of 4-fold rotation from the group O. The series of the axes $(L/m)_n = 4/(1+GCD(n-2,4)/2n)$ of this family of polytopes [5] (the greatest common divisor GCD (n-2, 4) = 4, 4, 1, 4, 2, 1) includes the axis 40/11 = 4/(1+1/10). Hence, along with the axis 40/11 of a single α-helix, the axes of this series also determine the approximants 40/11: 7/2, 11/3, 15/4, 18/5 that are the axes of the α-helices included in superhelices.

In the tube polytope ±[O×D_{20}], the two closest vertices of the helix {40/11} are the points of intersection of the lower and upper bases of the prismatic cell respectively with the left and right boundaries between the side face and the side faces adjacent to it. The intersection of the "side" (partitioning the side face of the cell) edges of the polytope with these boundaries defines on each of the boundaries two "boundary" polytope vertices belonging to two planes parallel to the base of the prismatic cell. The intersection of these planes with the "side" edges of the polytope allows one to define on the side face of the cell additional (not belonging to the polytope) vertices positioned between the closest vertices of the helix {40/11}. The helix {40/11} corresponds to the helix of atoms C_α in the α-helix; hence, positioning the atoms O, C', N, H (C' is the carbon atom between C_α and N) in the additional vertices of the side face of the cell leads to a "polytope" model of the peptide plane of the α-helix. The multiplication of this peptide plane by the screw axis 40/11 leads to the "polytope" model of the α-helix.

Conclusions

Ideal prototypes of α-helices and hydrocarbon chains of phospholipids of biomembranes are determined by the assembly of helices from building blocks—highly symmetric fragments of a four-dimensional 720-vertex polyhedron. This "block–polytope" approach allows us to explain the universality of the α-helix in proteins and the realization of a very limited number of hydrocarbon chains of phospholipids of biomembranes from a huge number of combinatorially possible variants of similar chains.

Acknowledgements

Corresponding author

* E-mail: talishome@mail.ru (A. L. Talis).

References

1. A. L. Rabinovich, A. L. Talis, *Bull. Russ. Acad. Sci.: Phys.*, **2021**, *85*, 863–867. DOI: 10.3103/S1062873821080220

2. E. I. Kats, M. I. Monastyrsky, *Phys. Scr.*, **2015**, *90*, 074003. DOI: 10.1088/0031-8949/90/7/074003

3. V. Elser, N. J. A. Sloane, *J. Phys. A: Math. Gen.* **1987**, *20,* 6161. DOI: 10.1088/0305-4470/20/18/016

4. H. S. M. Coxeter, *Regular Polytopes*, Dover, New York, **1973**.

5. L. Rastanawi, G. Rote, *arXiv: 2205.04965V1* [math.MG], **2022**. DOI: 10.48550/arXiv.2205.04965

6. S. Onaka, *Sci. Rep.*, **2024**, *14*, 18260. DOI: 10.1038/s41598-024-69108-w

7. A. L. Talis, A. L. Rabinovich, *Crystallogr Rep*., **2019**, *64*, 367–375. DOI: 10.1134/S106377451903026X

8. M. Samoylovich, A. Talis, *Acta Crystallogr.*, *Sect. A: Found. Adv.*, **2014**, *70*, 186–198. DOI: 10.1107/S2053273313033822

9. A. Talis, Y. Kucherinenko, *Acta Crystallogr*., *Sect. B: Struct. Sci.*, *Cryst. Eng. Mater*., **2023**, *79*, 537–546. DOI: 10.1107/S2052520623009393